

DEUTSCHES ELEKTRONEN-SYNCHROTRON
Ein Forschungszentrum der Helmholtz-Gemeinschaft



DESY 21-117
CERN-TH-2021-120
arXiv:2110.10711
October 2021

Dark Matter Freeze-In with a Heavy Mediator: Beyond the EFT Approach

E. Frangipane, S. Gori

Santa Cruz Institute for Particle Physics, University of California, Santa Cruz, USA
and

Department of Physics, University of California Santa Cruz, Santa Cruz, USA

B. Shakya

Deutsches Elektronen-Synchrotron DESY, Hamburg
and
CERN, Geneva, Switzerland

ISSN 0418–9833

NOTKESTRASSE 85 – 22607 HAMBURG

DESY behält sich alle Rechte für den Fall der Schutzrechtserteilung und für die wirtschaftliche Verwertung der in diesem Bericht enthaltenen Informationen vor.

DESY reserves all rights for commercial use of information included in this report, especially in case of filing application for or grant of patents.

To be sure that your reports and preprints are promptly included in the
HEP literature database
send them to (if possible by air mail):

<p>DESY Zentralbibliothek Notkestraße 85 22607 Hamburg Germany</p>	<p>DESY Bibliothek Platanenallee 6 15738 Zeuthen Germany</p>
--	--

Dark Matter Freeze-In with a Heavy Mediator: Beyond the EFT Approach

Evan Frangipane, Stefania Gori, Bibhushan Shakya

efrangip@ucsc.edu sgori@ucsc.edu bibhushan.shakya@desy.de

ABSTRACT:



—
—
—

$$L_\mu - L_\tau$$

—

— —

— — — —

-



—

— — —

=====

————— —————

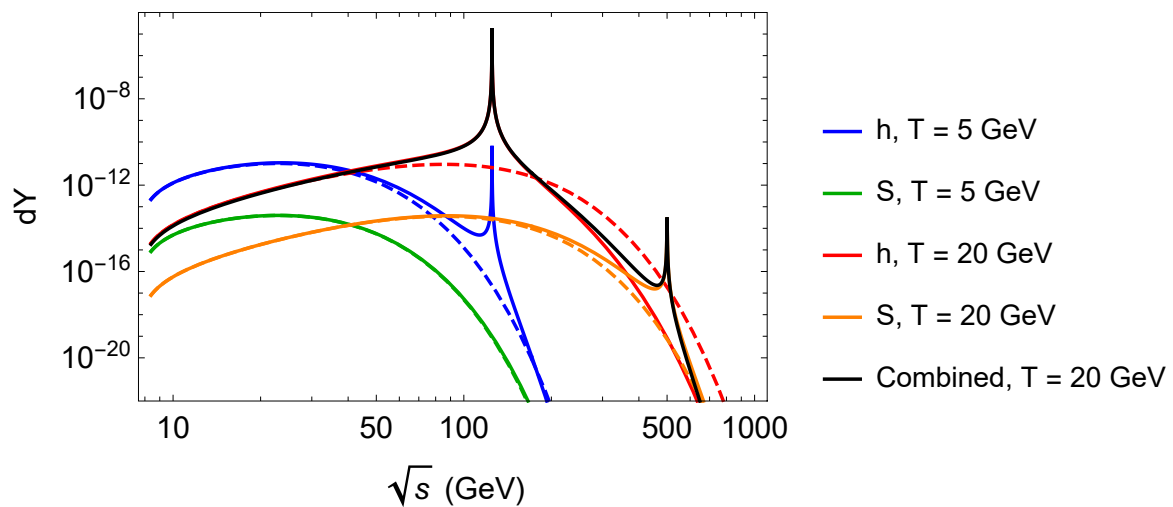
————— —————

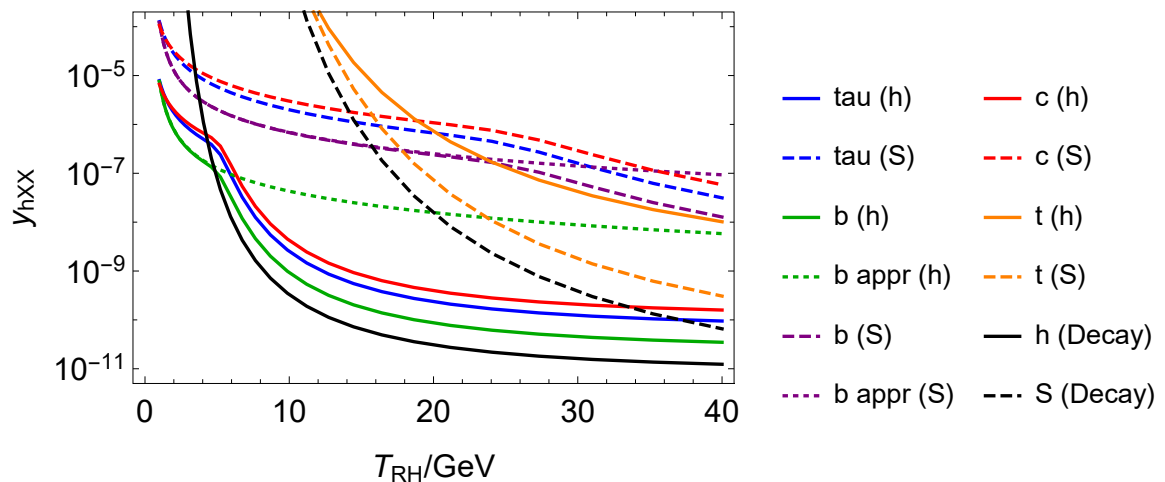
————— —————

————— —————

—————

—





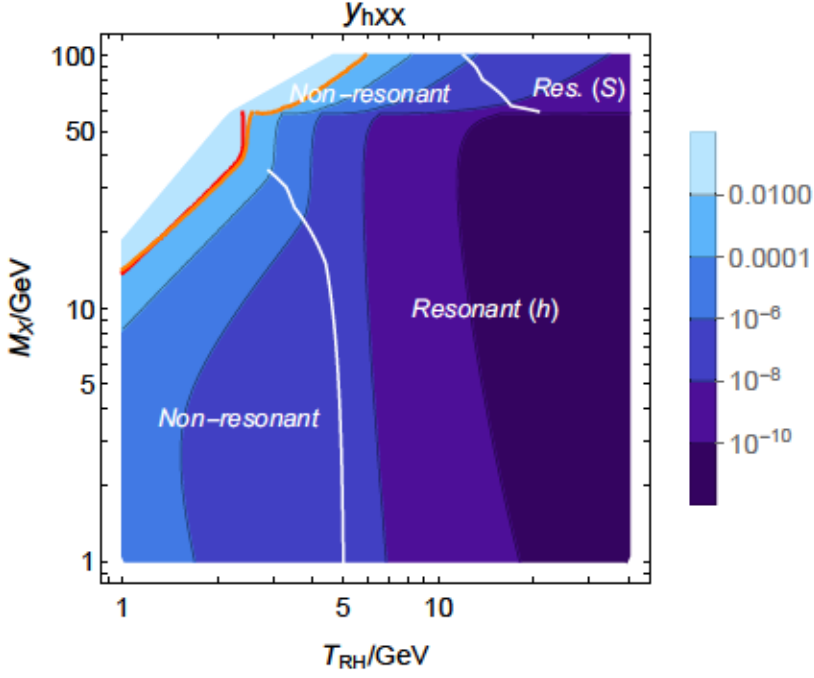


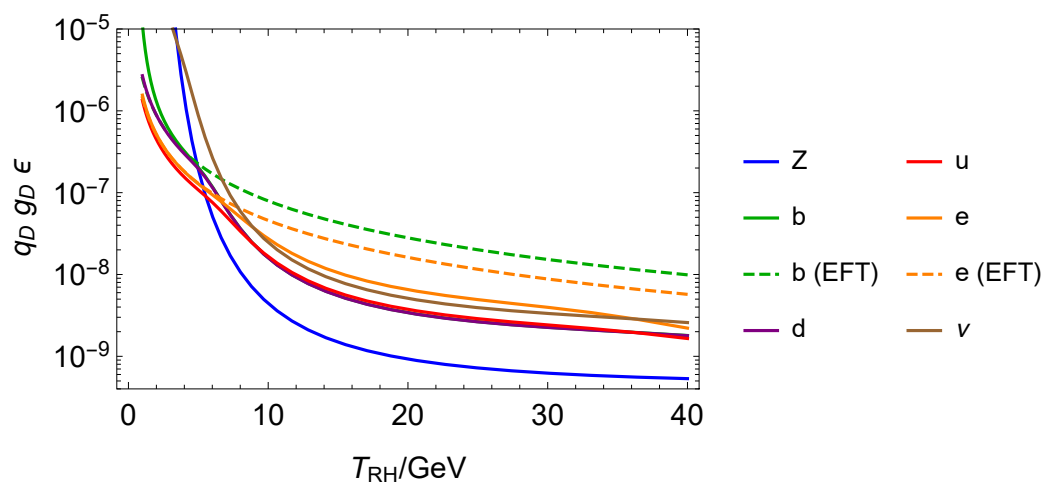
Figure 3. Contours of the Higgs-DM coupling (y_{hXX}) needed to produce the measured DM relic abundance, as a function of the reheat temperature and of the DM mass for $m_S = 500$ GeV and $\sin \theta_h = 0.1$. The white region corresponds to $y_{hXX} > 1$. The white curves separate regions of parameter space where different contributions dominate dark matter production, as specified by the labels. The red curve represents the LHC bound on Higgs invisible decays (see Sec. 5.1.1), whereas the orange curve represents the constraints from current direct detection data from XENON1T [31] (see Sec. 5.2).

be qualitatively similar to those in the previous (scalar) subsection, but with some crucial differences. In particular, in the kinetically mixed scenario, due to the dependence of the mixing angle on the ratio of the Z, Z' masses (see Eq. (2.5)), we will find that the heavier mediator as well as the interference term play a more important role. In the $L_\mu - L_\tau$ scenario, only the Z' contributes to the dark matter abundance.

3.2.1 Contributions to Dark Matter Freeze-In

In the EFT framework, the relevant interactions are derived from the four-fermion dimension-6 operators $\frac{1}{\Lambda_L^2} (\bar{f} \gamma_\mu P_L f)(\bar{X} \gamma^\mu X)$ and $\frac{1}{\Lambda_R^2} (\bar{f} \gamma_\mu P_R f)(\bar{X} \gamma^\mu X)$, with $P_{L,R}$ the left-handed and right-handed projection operators, respectively, and the coefficients $\Lambda_{L,R}$ given by

$$\frac{1}{\Lambda_{L,R}^2} = \frac{g_{L,R} g_X}{m_Z^2} + \frac{g'_{L,R} g'_X}{m_Z'^2}, \quad (3.5)$$



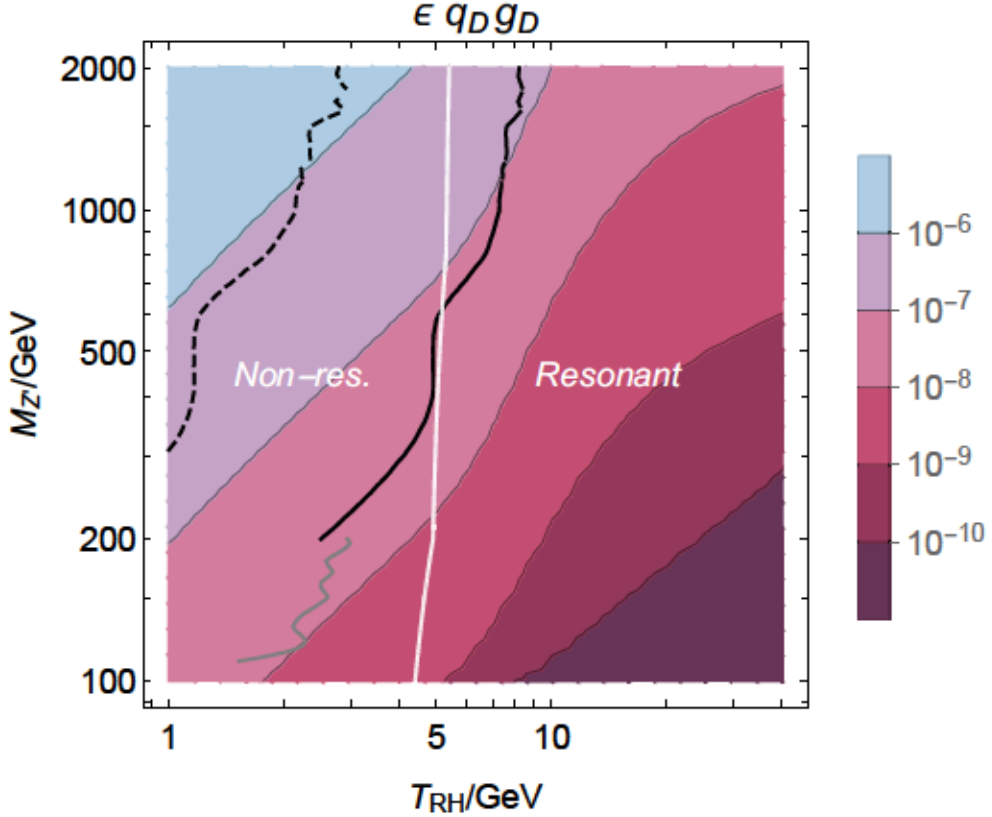
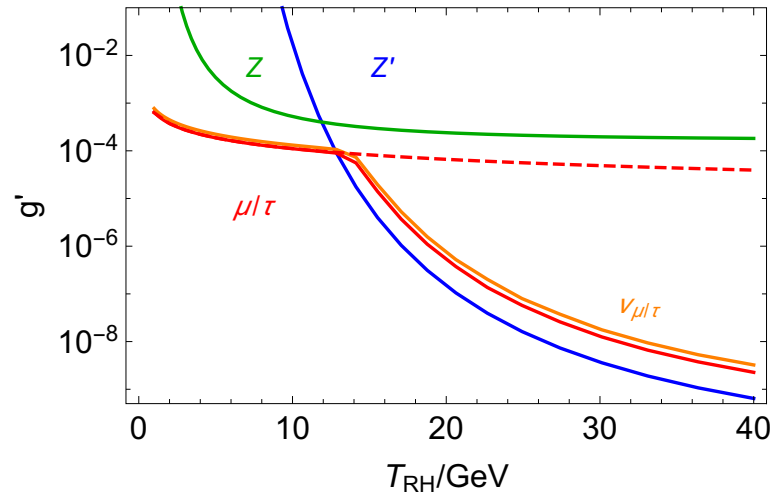


Figure 5. Value of $\epsilon q_D g_D$ needed to obtain the measured relic abundance as a function of $m_{Z'}$ and T_{RH} for $m_X = 1$ GeV. The white curve separates regions of parameter space where different contributions dominate dark matter production, as specified by the labels. We also show bounds from LHC searches for a heavy Z' decaying into a lepton pair: the grey curve represents the CMS bound [32]; the black curves represent the stronger bound between the ATLAS [33] and CMS [34] searches. For the LHC bounds, we fix $g_D q_D = 3 \times 10^{-6}$ (solid curves) and 3×10^{-5} (dashed curve).

sets of parameters, $g_D q_D = 3 \times 10^{-6}$ (solid curves) and 3×10^{-5} (dashed curve). Thus LHC constraints can be quite strong in the region of parameter space of interest if $g_D q_D$ is small.

3.2.3 Modified Vector Mediator: $L_\mu - L_\tau$

In this section, we study dark matter freeze-in in the $L_\mu - L_\tau$ model. The main difference between this framework and the kinetically mixed Z' model is that the heavy Z' mediator here couples directly to both dark matter and SM particles (muon and tau leptons and neutrinos) without requiring mixing with the SM Z boson. We have checked that processes mediated by the SM Z boson, which acquires a coupling to DM via loop-suppressed mixing effects (see Eq. (2.9)), are suppressed and negligible. Therefore, Z' mediated processes dominate the dark matter production and phenomenology.



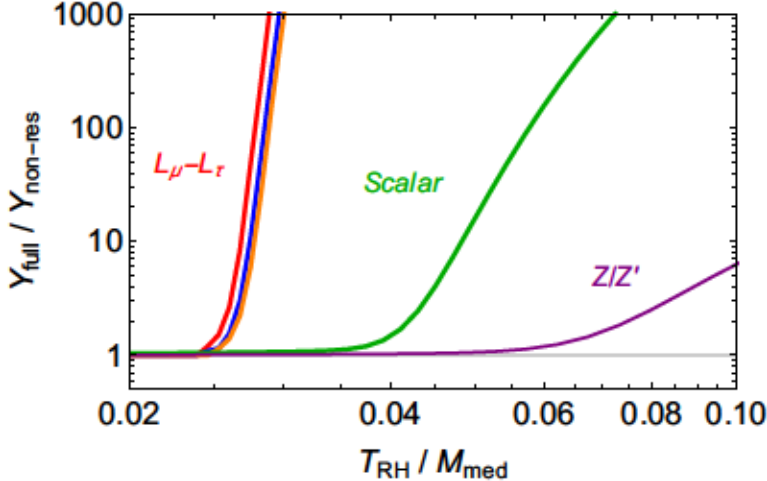
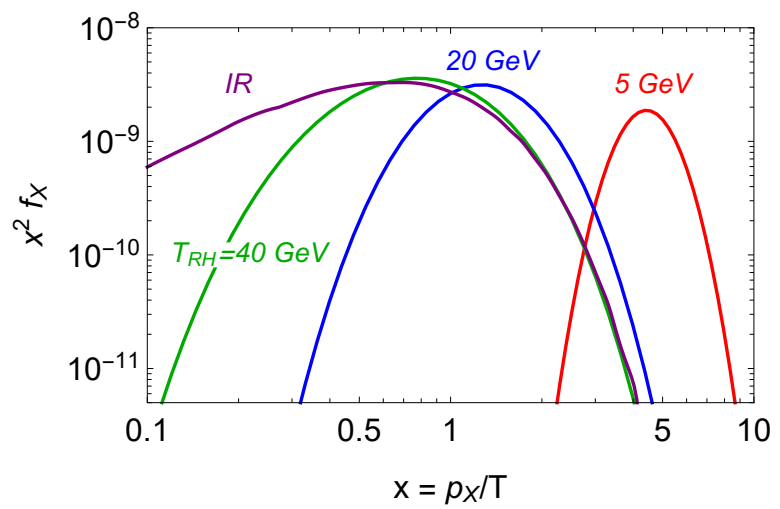
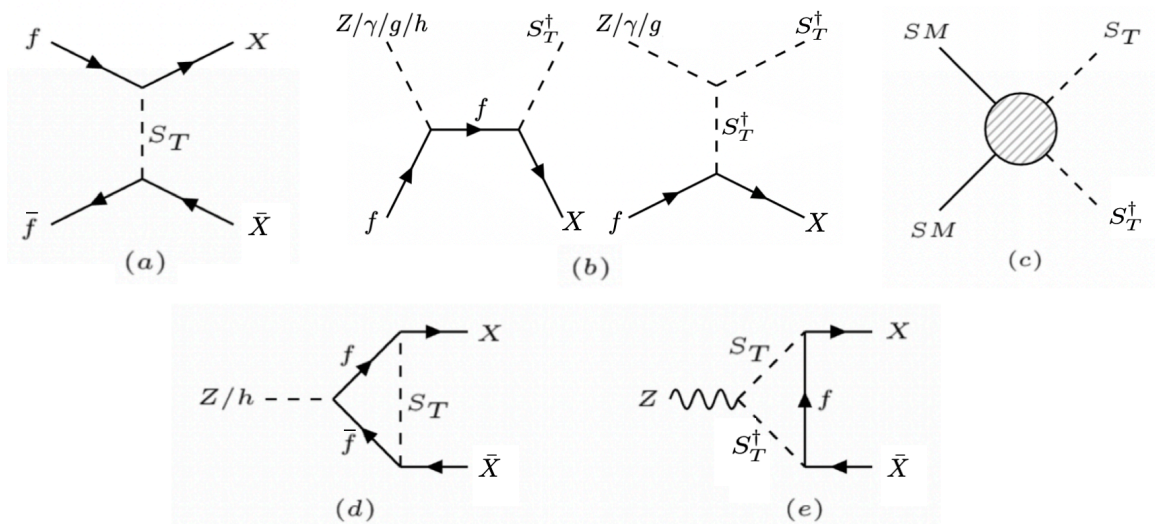


Figure 7. Ratio of the dark matter relic abundance from the full calculation to that obtained in the non-resonant EFT approximation, as a function of T_{RH}/M_{med} . From left to right, the curves are for the $L_\mu - L_\tau$ model with $M_{med} = m_{Z'} = 0.1, 1, 10 (red, blue, orange curves respectively), the scalar model (green curve, with $M_{med} = m_h$) and Z' kinetic mixing model (purple curve, with $M_{med} = m_Z$). For all curves, the couplings are chosen such that the full calculation gives the correct relic abundance for $m_X = 1.$$

We plot the ratio $Y_{full}/Y_{non-res}$, where Y_{full} is the dark matter relic abundance from the full calculation (including resonance effects), whereas $Y_{non-res}$ is the abundance obtained from the EFT approximations (obtained by dropping the s dependence in the denominators of the matrix elements). We use the values of the couplings that give the correct relic density for $m_X = 1 with the full calculation. This ratio is plotted as a function of T_{RH}/M_{med} , where M_{med} is the mass of the mediator that provides the largest contribution. From left to right, the curves are for the $L_\mu - L_\tau$ model with $M_{med} = m_{Z'} = 0.1, 1, 10 (red, blue, orange curves respectively), the scalar model (green curve, with $M_{med} = m_h$) and Z' kinetic mixing model (purple curve, with $M_{med} = m_Z$).$$

At low values of T_{RH}/M_{med} , $Y_{full}/Y_{non-res} \approx 1$ for all curves, showing that the EFT gives the correct dark matter relic abundance for sufficiently low T_{RH} in all cases. As T_{RH}/M_{med} increases, an increasingly larger fraction of the thermal distribution of SM fermions can access the s-channel resonance regime, resulting in deviations from the EFT calculations. Recall that the matrix elements scale as $|\mathcal{M}|^2 \sim 1/M_{med}^4$ in the non-resonant EFT limit but as $|\mathcal{M}|^2 \sim 1/M_{med}^2 \Gamma_{med}^2$ in the resonant regime. Therefore, the deviation from the EFT result is controlled by the magnitude of Γ_{med} relative to M_{med} : smaller widths, *i.e.* smaller values of Γ_{med}/M_{med} result in earlier deviations from the $Y_{full}/Y_{non-res} \approx 1$ limit. This is indeed visible in the plot: the Z' boson in the $L_\mu - L_\tau$ model has tiny couplings to the dark and SM particles, therefore a very narrow width, and thus begins to deviate from the EFT calculation already at $T_{RH}/M_{Z'} \approx 0.025$. The scalar curve deviates next at $T_{RH}/M_h \approx 0.035$, since the







— — — — — — —

— — — — — — —

— — — — — — —

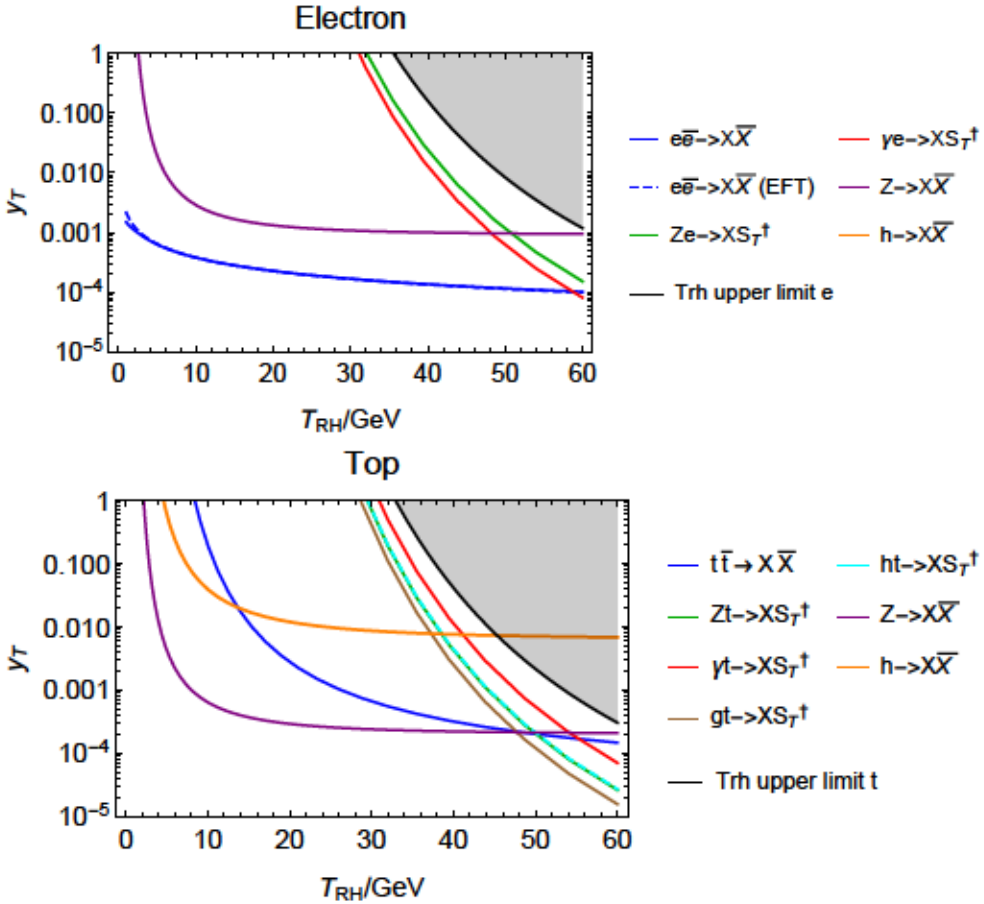


Figure 10. The size of the coupling y_T needed to produce the correct relic density from various processes as a function of the reheat temperature, T_{RH} , for S_T coupling to the right-handed electron e_R (top panel) and to the right-handed top-quark t_R (bottom panel), for $m_X = 1$ GeV and $m_{S_T} = 1200$ GeV. The dashed curve in the electron plot is the EFT approximation. In the shaded regions, coannihilation processes are rapid enough to produce a thermal DM population.

4.2 Cosmological History

We now turn to a discussion of the interplay between the above contributions in setting the correct dark matter relic density from freeze-in. Fig. 10 shows the relative contributions of the various channels as a function of T_{RH} for $m_X = 1$ GeV and $m_{S_T} = 1200$ GeV for scenarios where the mediator couples to e_R (top panel) or t_R (bottom panel). Here, we choose $m_{S_T} = 1200$ GeV for the mediator mass in view of strong constraints from LHC searches (see Sec. 5.1.3).

For the electron case (top panel of Fig. 10), the EFT approximation from Eq. (4.1) (dashed blue curve) closely matches the full calculation for $e^+e^- \rightarrow X\bar{X}$ (solid blue curve) throughout, as no strong resonance features are present for a t-channel mediator. The contribution from

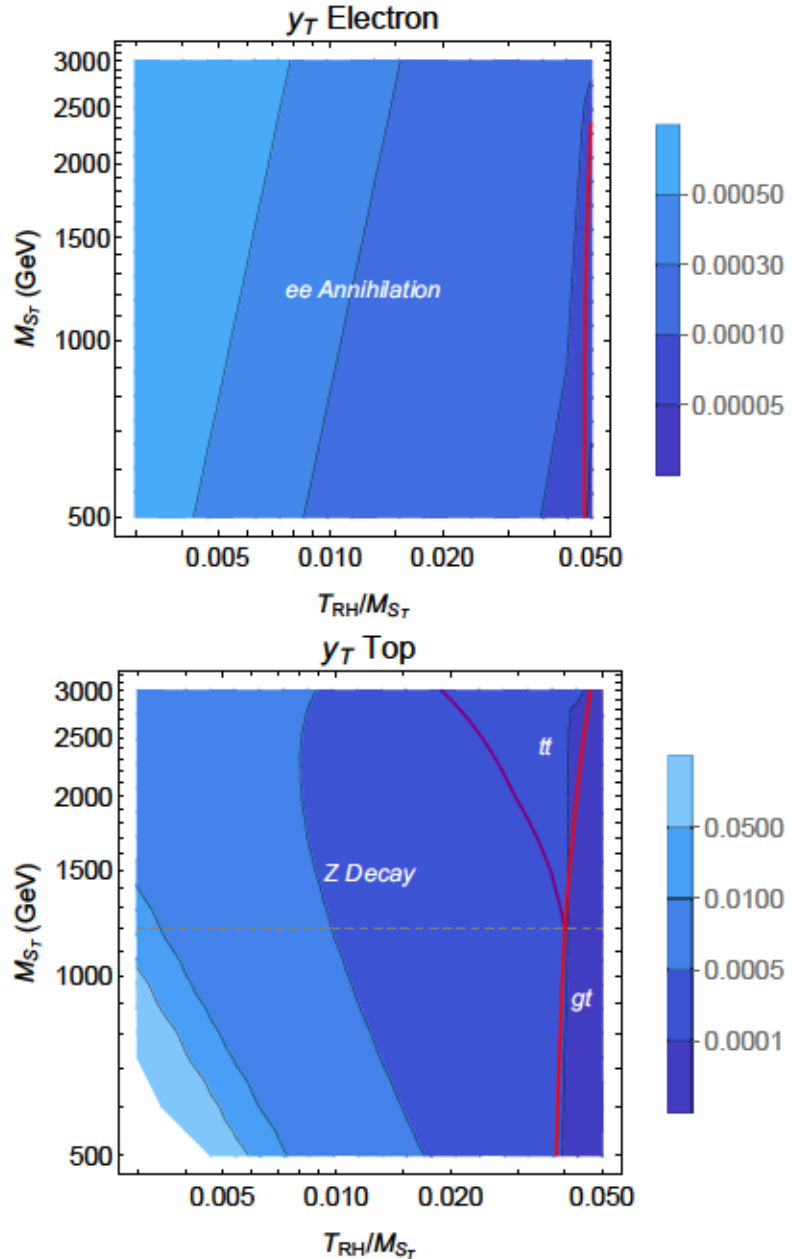


Figure 11. Contours of the coupling y_T needed to produce the correct relic density as a function of the reheat temperature, T_{RH} , and mediator mass, m_{S_T} , for $m_X = 1$ GeV, for scenarios where the mediator couples to the right-handed electron (top panel) or the right-handed top quark (bottom panel). Red curves separate regions where different processes dominate dark matter production, as denoted by the labels (see text for more details). The dashed grey curve in the bottom panel denotes the approximate lower bound on m_{S_T} from the LHC.

— —

$$L_\mu-L_\tau$$

— — —

— — — —
— — — —

[arXiv:hep-ph/0106249](#)

[arXiv:0911.1120 \[hep-ph\]](#)

[arXiv:1506.07532 \[hep-ph\]](#)

[arXiv:1712.07453 \[hep-ph\]](#)

[arXiv:1811.05478 \[hep-ph\]](#)

[arXiv:1809.10135 \[hep-ph\]](#)

[arXiv:1908.11387 \[hep-ph\]](#)

[arXiv:2102.06221 \[hep-ph\]](#)

[arXiv:1410.6157](#) [hep-ph]

[arXiv:2007.08768](#) [hep-ph]

[arXiv:1309.2777](#) [hep-ph]

[arXiv:1306.3996](#) [hep-ph]

[arXiv:1412.4791](#) [hep-ph]

[arXiv:1502.01011](#) [hep-ph]

[arXiv:1506.08195](#) [hep-ph]

[arXiv:1609.01289](#)

[hep-ph]

[arXiv:1609.06739](#) [hep-ph]

[arXiv:1908.05685](#) [hep-ph]

[arXiv:1306.4677](#) [hep-ph]

[arXiv:1912.06661](#) [hep-ph]

[arXiv:1806.00016](#) [hep-ph]

[arXiv:1803.01866](#) [hep-ph]

[arXiv:hep-ph/0206119](#)

[arXiv:1309.7348](#) [hep-ph]

[arXiv:1302.4438](#) [hep-ph]

[arXiv:1112.0493](#) [hep-ph]

[arXiv:hep-ph/0310123](http://arxiv.org/abs/hep-ph/0310123)

[astro-ph.CO]

[arXiv:1801.03509 \[hep-ph\]](http://arxiv.org/abs/1801.03509)

[arXiv:1805.12562](http://arxiv.org/abs/1805.12562)

[arXiv:1912.04776 \[hep-ex\]](http://arxiv.org/abs/1912.04776)

1

[arXiv:1903.06248 \[hep-ex\]](http://arxiv.org/abs/1903.06248)

1

<http://cds.cern.ch/record/2684757>

[arXiv:1503.01469 \[hep-ph\]](http://arxiv.org/abs/1503.01469)

[arXiv:1612.00009 \[hep-ph\]](http://arxiv.org/abs/1612.00009)

<http://cds.cern.ch/record/2743055>

[arXiv:1809.05937 \[hep-ex\]](http://arxiv.org/abs/1809.05937)

[arXiv:1902.00134 \[hep-ph\]](http://arxiv.org/abs/1902.00134)

[arXiv:1905.03764 \[hep-ph\]](http://arxiv.org/abs/1905.03764)

[arXiv:1610.07922 \[hep-ph\]](http://arxiv.org/abs/1610.07922)

<http://cds.cern.ch/record/2658263>

arXiv:2003.13744 [hep-ph]

arXiv:2102.10874 [hep-ex]

arXiv:1703.01651 [hep-ex]

arXiv:1006.0973 [hep-ph]

arXiv:1412.0018 [hep-ph]

arXiv:1808.03684 [hep-ex]

arXiv:1811.12446 [hep-ph]

arXiv:1403.1269 [hep-ph]

arXiv:1406.2332 [hep-ph]

arXiv:2004.14060 [hep-ex]

arXiv:2012.03799 [hep-ex]

arXiv:1912.08887 [hep-ex]

arXiv:2103.01290 [hep-ex]

[arXiv:1908.08215](#) [hep-ex]

[arXiv:2012.08600](#) [hep-ex]

[astro-ph.CO]

[arXiv:1904.00498](#)

[arXiv:1909.08632](#) [hep-ph]

[arXiv:1509.02910](#) [physics.ins-det]

[arXiv:1506.08309](#)

[physics.ins-det]

[arXiv:1803.05660](#)

[hep-ph]

[arXiv:hep-ph/9809453](#) [hep-ph]

[arXiv:hep-ph/0005123](#) [hep-ph]

[arXiv:1801.02640](#) [hep-ph]

[arXiv:1512.02751](#) [hep-ph]

[arXiv:1611.01517](#) [hep-ph]

[arXiv:1912.05581](#) [hep-ph]

[arXiv:1612.06840](#) [hep-ph]